AIP | Applied Physics Letters

Efficient broadband energy transfer via momentum matching at hybrid junctions of guided-waves

Charles Lin, Herman M. K. Wong, Benedict Lau, Mohamed A. Swillam, and Amr S. Helmy

Citation: Appl. Phys. Lett. **101**, 123115 (2012); doi: 10.1063/1.4753985
View online: http://dx.doi.org/10.1063/1.4753985
View Table of Contents: http://apl.aip.org/resource/1/APPLAB/v101/i12
Published by the American Institute of Physics.

Efficient broadband energy transfer via momentum matching at hybrid junctions of guided-waves

Charles Lin,[1] Herman M. K. Wong,[1] Benedict Lau,[1] Mohamed A. Swillam,[2] and Amr S. Helmy[1]
[1]*Department of Electrical and Computer Engineering, University of Toronto, Toronto M5S 3G4, Canada*
[2]*Department of Physics, The American University in Cairo, New Cairo 11835, Egypt*

(Received 2 August 2012; accepted 5 September 2012; published online 20 September 2012)

Momentum matching at hybrid junctions is examined for efficient broadband energy transfer between internal reflection guided waves and evanescence-based plasmonic-gap guided waves. We demonstrate a nanoscale orthogonal junction coupler between 50 nm air-filled plasmonic slot waveguides (PSWs) and 450 nm silicon rib waveguides. Non-resonant junction coupling efficiency of 50 ± 2 % between 1450 nm and 1650 nm is achieved experimentally and PSW propagation loss is directly measured to be only 2.5 dB/μm. This taperless hybrid junction reduces PSW-based device footprint and enhances device tolerance to temperature and fabrication process variations, serving as a potential platform for hybrid silicon-plasmonic interconnects. © *2012 American Institute of Physics*. [http://dx.doi.org/10.1063/1.4753985]

Nanoscale optical guided waves offer unique attributes that stem from their ability to localize field at the subwavelength scale. It has been shown recently that such localization in plasmonic slot waveguides (PSWs) can alleviate some of the bottlenecks in current very large scale integrated circuit technologies[1–3] and serves as an effective platform for the realization of optoelectronic devices on Si that enables the next generations of optical interconnects. Their small footprint, versatile functionality, low parasitics, and hence high speed and low power consumption are some of the advantages offered by this platform. Significant light attenuation due to metal absorption inhibits, however, the possibility of using PSW as an on-chip signal transmission bus for more than a few microns. A practical solution for the interconnect bottleneck may well use a hybrid approach for the design, where the PSWs are utilized for high density integration of functional devices for signal processing, while conventional Si waveguides can still serve as low-loss signal transmission medium between these devices and electronic circuits.

The lack of efficient coupling mechanism between dielectric waveguides and PSWs, however, is a formidable challenge which impedes the feasibility of practically utilizing the hybrid platform. The PSW mode is a coupled surface wave confined within a sub-100 nm core where the field intensity is highest at the metal-dielectric interfaces and decays exponentially into the metal claddings. On the other hand, diffraction-limited dielectric waveguide has a modal area of few hundreds of nanometers and is based on total internal reflections (TIR) with field intensity that peaks at the center of the waveguide core. Consequently, their momentum distribution, dispersion, and modal profile are all fundamentally different. These diverse distinctions pose fundamental obstacles to interface and utilize the two classes of modes simultaneously in the nanoscale.

Efficient energy transfer between TIR-based waveguides and PSWs can be achieved by direct end-fire coupling with stub structures that reduce the momentum mismatch.[4] However, this design has limited bandwidth due to resonance effect associated with the stubs and is also subject to low fabrication tolerance. This bandwidth constraint can be eliminated by introducing an intermediate taper region between the two waveguides. Nonetheless, tapering a dielectric waveguide to sub-100 nm would result in plane wave-like mode with modal area significantly larger than that of PSWs. On the other hand, air-core plasmonic (metallic) tapers or adiabatic dielectric tapers enclosed by metal claddings interface well with Si waveguides and can resolve the modal mismatch bottleneck.[5] However, the micron-sized metallic taper leads to an increase in the overall device footprint and its intrinsic loss drastically reduces the amount of power delivered into the plasmonic slot. A strategy to eliminate the taper region may be to use the direct end-fire scheme to first couple from the Si waveguide to a PSW with comparable core width and then utilize a $\lambda/4$ transformer to transfer the optical power into the subwavelength PSW.[6] Nonetheless, such abrupt coupling scheme is still limited by the modal shape and momentum mismatch. Thus, an alternative coupling mechanism without taper structures is still lacking and is of prime importance to enable the simultaneous utilization of these two classes of waveguides.

In this paper, we demonstrate a momentum matching technique that enables efficient energy transfer between 450 nm wide Si waveguides and 50 nm wide PSWs through an orthogonal junction with record nanoscale footprint and broadband performance. Detailed design, fabrication, and spectroscopic characterization of this orthogonal hybrid junction are discussed. The performance assessment was carried out over a wide bandwidth between 1450 and 1650 nm. The efficient PSW excitation in the orthogonal junction and the non-resonant and ultra-wide bandwidth of this platform are experimentally confirmed. The experimental measurements match closely with the simulation results, thus confirming the design's tolerances against temperature drift and fabrication imperfections. This coupling scheme provides the optimum interface between low-loss silicon technology and subwavelength plasmonic structures, ushering in a new era for a wide range of silicon-plasmonic hybrid interconnect devices and associated applications.

The efficiency of energy coupling at any guided wave junction discontinuity is governed by the momentum mismatch and the spatial overlap of modes at either end of the junction. Careful examination of the modal field inside the Si waveguide shows that an efficient mechanism to directly interface the two classes of waveguides is to alter the junction configuration used in the end-fire scheme. In Fig. 1, the mismatch between the longitudinal momentum component of Si waveguide (K_l^{Si}) and the momentum component of a 50 nm PSW with Ag claddings (K_l^{SPP}) is described by the δK_1 plane whereas the mismatch between the transverse momentum component of Si waveguide (K_t^{Si}) and K_l^{SPP} is described by the δK_2 plane. Due to the significant modal index difference between Si waveguide and PSW, δK_1 does not intersect with the plane of zero momentum mismatch ($\delta K = 0$). Thus, momentum matching is not possible without stub or taper structures. On the other hand, intersection between the δK_2 and $\delta K = 0$ planes indicates that it is possible to directly achieve the momentum matching condition. This can be done by placing the two waveguides in an orthogonal configuration and results in a good coupling efficiency as shown in Fig. 2. This coupling mechanism is analogous to the Otto configuration of coupling to surface plasmons where a prism is used to minimize the momentum mismatch between the incident plane wave and the single surface plasmon.[7] The momentum matching condition can be tuned for different wavelengths by changing the incident angle of the plane wave. Similarly, in the proposed orthogonal configuration, K_t^{Si} with K_l^{SPP} are aligned such that the momentum mismatch vanishes at a certain wavelength. The wavelength at which the mismatch vanishes can be tuned by controlling the width of the Si waveguide (Fig. 1).

Although the momentum matching condition is only satisfied at a single wavelength (Fig. 1), the rate of change of δK_2 with respect to wavelength is small. Since PSW spatial modal characteristics are almost invariant for PSW with subwavelength core, a good coupling efficiency could be achieved over a wide spectrum. Thus, broadband, non-

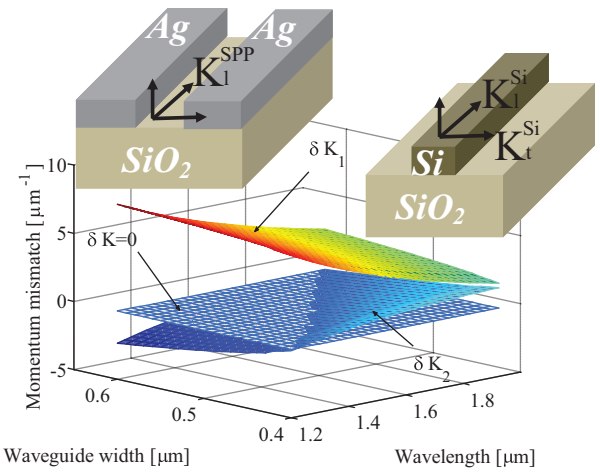

FIG. 1. (a) The momentum mismatch between Si waveguide and 50 nm PSW with Ag claddings is plotted as a function of wavelength and Si waveguide width. The waveguides are 340 nm tall and on a 1 μm SiO_2 substrate. Johnson and Christy material model is used in an in-house finite-difference mode solver to extract momentum vectors. The mismatch between K_l^{SPP} and K_l^{Si} is designated as δK_1 and the mismatch between K_l^{SPP} and K_t^{Si} is designated as δK_2.

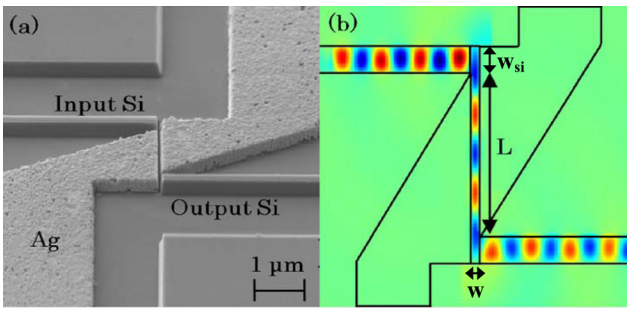

FIG. 2. (a) Scanning electron microscope image of an orthogonal hybrid junction platform between Si wires (w_{Si} = 450 nm) and PSW with Ag claddings ($w = 50$ nm, $L = 1$ μm). The device is 340 nm tall and sits on 1 μm SiO_2 substrate. (b) The magnitude of the propagating transverse-magnetic field on the same platform at $\lambda = 1550$ nm obtained through 3D simulation using Lumerical software.

resonant, and highly efficient energy transfer between PSWs and Si waveguides can be readily achieved. The linear slope of the δK_2 plane also ensures that the ultra-wide bandwidth remains invariant when the width of the Si waveguide is fine-tuned to maximize the coupling efficiency at a specific operating wavelength. In addition to matching the momentum, the orthogonal configuration increases the effective area of the PSW that interfaces with the TIR mode of the Si waveguide, thereby increasing the spatial modal overlap necessary for efficient coupling. Thus, tapers are no longer required and a nanoscale coupler footprint can be achieved. Based on 3D FDTD simulations using Lumerical software, the proposed hybrid junction has a coupling efficiency of 70% and the overall platform consisted of both input and output hybrid junctions has a 3 dB bandwidth of 996 nm (Fig. 3 inset).[8] If the width of the PSW slot is increased, the coupling efficiency can be even higher since the modal intensity would shift towards the dielectric region, which further reduces the modal shape mismatch.

To experimentally demonstrate the capability of the orthogonal coupling scheme, hybrid junctions between 50 nm PSWs with Ag claddings and 450 nm Si waveguides are fabricated. The waveguides are fabricated via electron beam lithography and the PSW slots are milled using focused ion beam (FIB). The nominal width of the Si waveguides is designed to be 450 nm to achieve phase matching condition

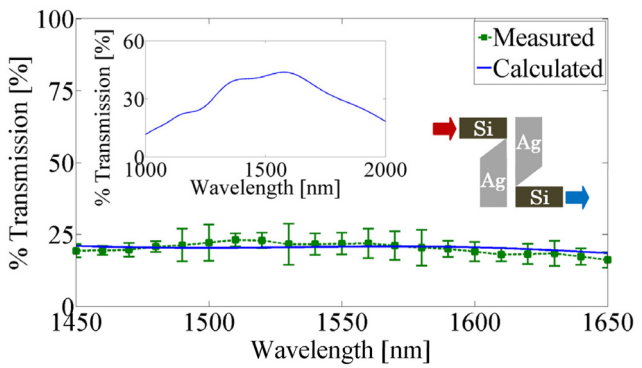

FIG. 3. Comparison between experimental and theoretical bandwidth of orthogonal junction platform between Si wires (w_{Si} = 450 nm) and PSW with Ag claddings ($w = 50$ nm, $L = 400$ nm). The theoretical calculation accounts for the trapezoidal waveguide sidewalls. (Inset) Theoretical bandwidth of the same platform with vertical Si waveguide sidewalls.

at 1550 nm. Straight Si waveguides are placed next to the hybrid junctions as reference for loss measurement calibration. Based on Fabry-Perot loss measurements, the average propagation loss of the Si waveguides at 1550 nm is 8.02 ± 2.34 dB/cm. The significant waveguide loss can be attributed to surface roughness as well as light absorption due to the deposition of scattered Ag particles onto the Si waveguide sidewalls during the FIB process.

To demonstrate the ultra-wide bandwidth of the orthogonal junction platform, a wavelength sweep of 200 nm is performed on 8 hybrid platforms with 400 nm long PSWs (Fig. 3). The percent transmission of the hybrid platform is calculated by normalizing the power transmitted through the fabricated device, which includes both the platform and the input/output Si waveguides, with respect to the power transmitted through a reference straight Si waveguide. This is to eliminate the effect of propagation loss in Si waveguides used to couple light in and out of the platform. The theoretical percent transmission of the platform is displayed in the inset, which is around 50% at $\lambda = 1550$ nm. Nonetheless, the experimental percent transmission plotted in the main graph is close to 23%. The discrepancy is attributed to fabrication imperfections that cause Si waveguides to have slanted sidewalls at 27°. This creates air gap between PSW and Si waveguides and degrades the coupling efficiency at each junction. The theoretical bandwidth calculated based on simulation that uses trapezoidal Si waveguide profile is also plotted in Fig. 3 and matches well with the experimental result, thereby confirming the origin of the reduction in power transmission. Despite the performance degradation, the overall power transmission is observed to be non-resonant, constant, and only drops by less than 3% across the 200 nm bandwidth.

With PSWs of different lengths, the coupling efficiency of the orthogonal junction can be extracted using the cutback method. By plotting the logarithm of the power transmitted through the fabricated devices as a function of PSW length, the coupling efficiency can be extracted from the y-intercept of the fitted curve. The coupling efficiency is assumed to be identical for input and output junctions and is defined as the combination of the amount of power transmitted from Si waveguide into PSW and the coupling between the two modes. The transmission spectrum at $\lambda = 1550$ nm is plotted in Fig. 4, where the coupling efficiency of a single hybrid

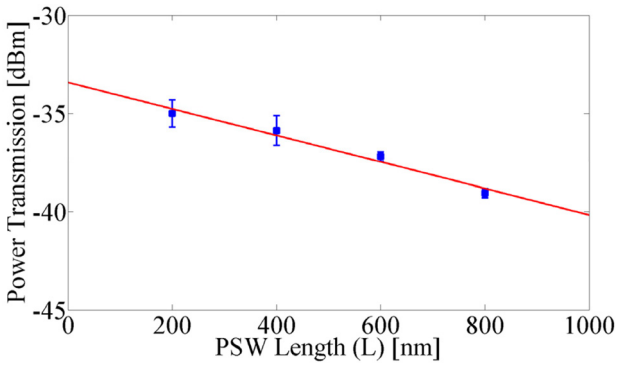

FIG. 4. The power transmission through PSWs ($w = 50$ nm) at $\lambda = 1550$ nm is plotted as a function of PSW length. The slope of the linear fit conveys information on PSW propagation loss, while the intercept at $L = 0$ is used to extract the coupling efficiency of the orthogonal junction.

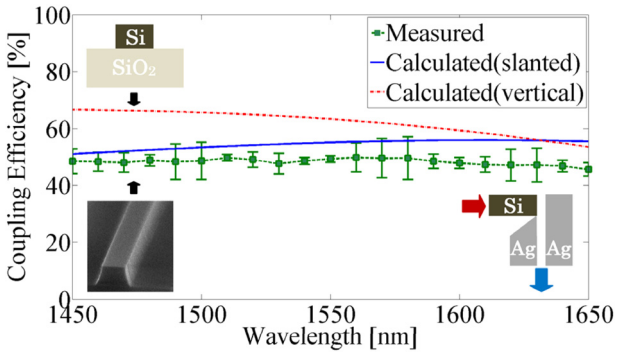

FIG. 5. The coupling efficiency of a single hybrid orthogonal junction (inset) is plotted as a function of wavelength. The solid and dash lines represent the calculated coupling efficiency simulated using trapezoidal and rectangular Si waveguide, respectively.

junction is determined to be $50.6 \pm 2\%$. The result slightly deviates from the theoretical value of 55% due to the air gaps between PSW and Si waveguides and the misalignment in the lithography process of up to 50 nm. Nonetheless, the coupling efficiency of the hybrid junction is invariant over the 200 nm bandwidth with standard error of the mean of less than 10% (Fig. 5).

In addition to the coupling efficiency of the hybrid junction, the PSW propagation loss can also be extracted from the cutback method and is related to the slope of the fitted linear curve. Based on the result in Fig. 4, the average PSW propagation loss at $\lambda = 1550$ nm is calculated to be 2.5 ± 0.3 dB/μm with small variations across samples. The propagation loss over the 200 nm bandwidth is displayed in Fig. 6 and shows good agreement with numerical predictions, where the waveguide loss increases at lower wavelength. However, the experimental values are slightly higher than the theoretical values with variations of less than 1 dB. Additional loss mechanisms such as porosity in the Ag film and angled slot waveguide sidewalls created by the narrowing of the FIB beam waist during the sputtering process all contribute to the increase in PSW loss. Furthermore, the amount of misalignment in the lithography process is larger for junctions with shorter PSWs. This can be observed in the larger measurement variation associated with shorter PSWs shown in Fig. 4. The variation in the amount of misalignment introduces additional error when waveguide propagation loss is extracted based on the

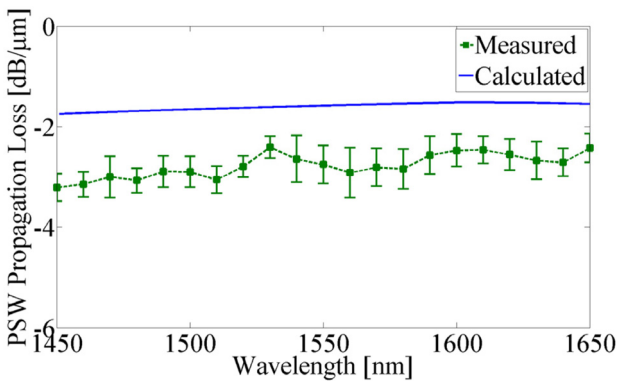

FIG. 6. The propagation loss of air-filled PSW ($w = 50$ nm) with Ag claddings is plotted as a function of wavelength.

cutback method. Nonetheless, our result is comparable to previously reported loss value[9] where the PSW slot was made wider and filled with poly(methyl methacrylate) to alleviate the waveguide loss.

The insertion loss and junction coupling efficiency of our hybrid platform are nearly invariant across the 200 nm bandwidth. This not only demonstrates a coupling scheme with potential for high bit-rate interconnect applications, but also indicates that the design is temperature insensitive and has high fabrication tolerance. The average on-chip temperature of an integrated circuit die is often non-uniform depending on the surrounding circuitries, typically fluctuating between several tens of degrees.[10] This temperature fluctuation can alter the lasing wavelength of on-chip laser diode by up to 5 nm.[11] Moreover, nanoscale functional devices based on cascaded networks of PSW junctions have recently been proposed for various wavelength-selective routing applications.[12,13] These PSW devices operate based on resonance and interference effects and are thus highly sensitive to changes in effective index of the waveguide, which is also critically dependent on temperature fluctuations. With ultrawide and non-resonant bandwidth, the orthogonal junction enables an efficient coupling scheme that is capable of accommodating large temperature changes as well as drift in laser and device operation wavelength. Moreover, since changes in waveguide dimensions can be correlated to changes in the operating wavelength, the wideband coupler characteristic also ensures that the performance of PSW devices is immune to variations in fabrication processes.

In addition to strong temperature and fabrication tolerances, efficient coupling in our orthogonal scheme is achieved in minimal spatial dimensions at the PSW-Si interface. This in turn allows the nanoscale confinement of the PSW to be truly utilized for reducing optical device footprint. With a coupling mechanism in place that enables an efficient interface between dielectric waveguides and PSWs, it is now possible to pursue hybrid design of optical network with PSW as the building block for signal manipulation and TIR-based waveguide for communication between devices. The hybrid design strategy can reduce the footprint of photonic devices by at least an order of magnitude to a scale of integration approaching that of electronics.[12] Although this coupling scheme is demonstrated for air-filled PSWs, it is a generalized method that is also applicable to PSWs that are filled with polymers and gain media for active and nonlinear applications. This allows PSW to serve as a versatile candidate for optical interconnect on the chip level of integrated circuits. Furthermore, with orthogonal waveguide placement, vertical and 3D waveguide integrations are also possible. Finally, the constant waveguide propagation loss near 1550 nm further validates the applicability of PSW for the design of telecommunication devices.

In summary, we have demonstrated a highly efficient, non-resonant, and broadband scheme of interfacing Si and plasmonic technologies using orthogonal junctions. The tunable mechanism by which this performance is achieved utilizes momentum matching between the two classes of waveguides at a nanoscale junction without taper structures. Using this coupling technique, the coupling efficiency at each junction is experimentally confirmed to be constant over a 200 nm bandwidth and the theoretical 3 dB bandwidth can be up to 996 nm. The wide bandwidth, low sensitivity to fabrication process variations, and compact footprint of this coupling scheme are the driven advantages to exploit such junction in realizing temperature-insensitive functionalities for high-bandwidth silicon-plasmonic interconnect applications.

[1]H. A. Atwater, Sci. Am. **296**, 56 (2007).
[2]D. K. Gramotnev and S. I. Bozhevolnyi, Nature Photon. **4**, 83 (2010).
[3]J. A. Dionne, L. A. Sweatlock, and H. A. Atwater, Phys. Rev. B **73**, 035407 (2006).
[4]G. Veronis and S. H. Fan, Opt. Express **15**, 1211 (2007).
[5]P. Ginzburg, D. Arbel, and M. Orenstein, Opt. Lett. **31**, 3288 (2006).
[6]P. Ginzburg and M. Orenstein, Opt. Express **15**, 6762 (2007).
[7]A. Otto, Z. Phys. **216**, 398 (1968).
[8]B. Lau, M. A. Swillam, and A. S. Helmy, Opt. Express **18**, 27048 (2010).
[9]Z. Han, A. Y. Elezzabi, and V. Van, Opt. Lett. **35**, 502 (2010).
[10]Y. Vlasov, W. M. J. Green, and F. Xia, Nature Photon. **2**, 242 (2008).
[11]S. Sakamoto, H. Kawashima, H. Naitoh, S. Tamura, T. Maruyama, and S. Arai, IEEE Photon. Technol. Lett. **19**, 291 (2007).
[12]C. Lin, M. A. Swillam, and A. S. Helmy, "Analytical Model for Metal-Insulator-Metal Mesh Waveguide Architectures," J. Opt. Soc. Am B (to be published).
[13]M. A. Swillam and A. S. Helmy, IEEE Photon. Technol. Lett. **24**, 497 (2012).